*Journal of Applied Electrochemistry* **34**: 1229–1233, 2004.
© 2004 *Kluwer Academic Publishers. Printed in the Netherlands.*


# The relationship between the structure and electrocatalytic properties of $TiO_2$ electrodes doped with $CeO_2$

CÉLIA MACHADO RONCONI[1], PAULO ROBERTO ZANOTTO[2], URSULA BROCKSOM[2], PEDRO A.P. NASCENTE[3] and ERNESTO CHAVES PEREIRA[1,*]

[1]*Centro Multidisciplinar para o Desenvolvimento de Materiais Cerâmicos (CMDMC), Departamento de Química, Universidade Federal de São Carlos, Caixa Postal 676, 13560-970 São Carlos, SP, Brazil*

[2]*Laboratório de Química Orgânica Sintética, Universidade Federal de São Carlos, Caixa Postal 676, 13560-970 São Carlos, SP, Brazil*

[3]*Departamento de Engenharia de Materiais Universidade Federal de São Carlos, Caixa Postal 676, 13560-970 São Carlos, SP, Brazil*

*(*author for correspondence, e-mail: decp@power.ufscar.br)*

Received 10 February 2004; accepted in revised form 12 July 2004

*Key words:* $CeO_2$, electrocatalysis, nitrobenzene electroreduction, oxide electrodes, Pechini method, $TiO_2$

**Abstract**

This paper describes the study of the preparation of $Ti/Ti_{1-x}Ce_xO_2$ electrodes using the Pechini method and their application for the electroreduction of nitrobenzene in aqueous acid medium. The electrodes were studied using X-ray diffraction, and scanning electron microscopy and it was found that the electrocatalytic properties are influenced by the microstructure and morphology of the electrodes. All doped electrodes presented an enhanced performance for nitrobenzene electroreduction when compared to pure $TiO_2$. The $Ti_{0.995}Ce_{0.005}O_2$ electrode presented the best performance, with an increase of 58% in the aniline yield under galvanostatic electrolysis conditions.

## 1. Introduction

Since the discovery of dimensionally stable anodes (DSA®) by Beer in the 1960s, many new electrode materials have been developed [1–5]. DSA® materials consist of a metallic substrate with a ceramic coating whose basic composition is a mixture of $RuO_2$ ($IrO_2$) + $TiO_2$ in which $RuO_2$ provides the catalytic properties and $TiO_2$ is responsible for the mechanical and chemical stability [5].

However, in other applications, $TiO_2$ can also present electrocatalytic properties itself. In this sense, several papers have reported the electroreduction of different nitro-compounds on $Ti/TiO_2$ electrodes [6–12]. The mechanism proposed for these reactions involves the reoxidation of $Ti^{3+}$ sites to $Ti^{4+}$, associated with the reduction of nitro-compound molecules adsorbed on the surface [10]. For example, the electroreduction of *o*-nitrophenol, in acid medium, occurs as follows [10]:

$$6Ti^{3+} + NO_2C_6H_4OH + 6H^+ \leftrightarrow 6Ti^{4+} + NH_2C_6H_4OH + 2H_2O \quad (1)$$

In a previous study carried out in this laboratory, the systematic investigation of the electrocatalytic properties of $Ti/TiO_2$ electrodes for nitrobenzene reduction [13] was performed. A factorial design was employed to evaluate the effects of the preparation variables and their relation to the electrocatalytic reduction of nitrobenzene on $TiO_2$ electrodes. Electrodes were prepared by the Pechini method, which consists of the synthesis of a polyester with the metal salt dissolved in it [14]. This methodology permits the preparation of oxides with low level doping and, in the case of powders, the formation of nanoparticles [15].

In this work, attention has been focused on modifying $Ti/TiO_2$ electrodes by incorporation of cerium oxide. This was achieved with the aim of improving the electrode activity for nitrobenzene reduction. $CeO_2$ was selected because it promotes an enhancement of the electrochemically active surface area in DSA materials [16]. Structural, morphological and compositional information was obtained using X-ray diffraction, and scanning electron microscopy. The surface area was obtained in order to investigate textural properties. Finally, a correlation between the electrochemical and physical properties of the electrodes is proposed.

## 2. Experimental

The $Ti_{1-x}Ce_xO_2$ and the $TiO_2$ electrodes were prepared on Ti substrates. In previous studies, it was shown that

the best $TiO_2$ electrode for nitrobenzene (NB) electroreduction, prepared by Pechini method, was obtained using a precursor molar composition of 1:2:8 (tetraisopropoxide of titanium:citric acid:ethylene glycol) and this was the composition used in the present study [13].

In order to modify the oxide properties, different concentrations of $(NH_4)_2Ce(NO_3)_6$ (Reagen) were added to the precursor. The oxide electrodes were prepared with the following contents of $CeO_2$: 0.10, 0.25, and 0.50 mol%. The precursors were painted on both sides of the Ti substrates, and polymerized at 130 °C for 15 min. The samples were then treated at 250 °C for 15 min, in order to improve the adhesion of the oxides. Finally, the electrodes were annealed at 450 °C for 15 min. The entire procedure was repeated ten times to increase the film thickness.

The samples were characterized by X-ray diffraction (XRD) using a Siemens D5000 diffractometer, with a CuK$\alpha$ source ($\lambda = 1.5406$ Å). Microstructural analysis was performed using a Zeiss DSM 940A scanning electron microscope.

Electrochemical measurements were carried out with an EG & G PARC potentiostat/galvanostat model 273 A. These experiments were performed in a single compartment electrochemical cell. A semicircular platinum foil counter-electrode ($A = 21.2$ cm$^2$), a saturated calomel reference electrode (SCE) and the working electrode were placed in a 0.50 mol dm$^{-3}$ $H_2SO_4$ (Merck) aqueous solution at 25 °C. Prior to the electrochemical measurements, pure nitrogen was bubbled through the solution for 30 min.

Galvanostatic electrolyses of nitrobenzene (NB) in aqueous 0.50 mol dm$^{-3}$ $H_2SO_4$ solution were carried out in a three compartment glass cell under stirring ($V = 200$ cm$^3$). In order to prevent product crossover from the cathodic compartment to the anodic one, the anodes were placed in two side compartments and separated from the main compartment by a sintered glass barrier. Platinum electrodes ($A = 1$ cm$^2$) were used as anodes. The Ti/$Ti_{1-x}Ce_xO_2$ electrode was positioned in the main compartment. The galvanostatic electrolyses were performed using a homemade dc source. A current density of 10 mA cm$^{-2}$ was used and the temperature was kept constant at 50 °C ($\pm 1$ °C). Pure nitrogen was bubbled through the solution before each measurement. Finally, the reaction products were analyzed by gas chromatography (Shimadzu model GC 17) using a DB1-30 m column.

## 3. Results and discussion

### 3.1. *Structural, and morphological characterization*

The $Ti_{1-x}Ce_xO_2$ ($x = 0$, 10, 0.25 and 0.50 mol%) films were light-yellow colored, and presented good adherence to the Ti substrates. The XRD patterns of films with different contents of $CeO_2$ reveal only the presence of the anatase phase. The crystallite size ($D$) of $Ti_{1-x}Ce_xO_2$ films was estimated by Scherrer's equation [17] using the strongest peak FWHM and the results are presented in Table 1. As can be observed, the presence of $CeO_2$ leads to a significant modification of the crystallite size of the $TiO_2$ electrodes. This means that the addition of $CeO_2$ into the $TiO_2$ lattice inhibits grain growth.

*Table 1.* Crystallite size of the $Ti_{1-x}Ce_xO_2$ Samples

| $Ti_{1-x}Ce_xO_2$ | D (nm) (film) |
|---|---|
| $x = 0.00$ mol% | 18 |
| $x = 0.10$ mol% | 14 |
| $x = 0.25$ mol% | 13 |
| $x = 0.50$ mol% | 10 |

As only low levels of doping are used in this study, the $Ce^{4+}$ ions can be incorporated in the $TiO_2$ lattice or segregated as a secondary phase. Generally, due to difference in the ionic radii and in the lattice structure ($TiO_2$ (orthorhombic) and $CeO_2$ (cubic)), an extensive solid solution is not formed. However, in the low-range doping investigated in this work, a solid solution can be formed. Leite et al. [18] demonstrated that the solubility of doping ions increases as the grains size decreases. Therefore, considering the XRD results, it is possible that the incorporation of small quantities of $Ce^{4+}$ into the $TiO_2$ lattice can result in a solid solution of $Ti_{1-x}Ce_xO_2$, according to following reaction (using Kröger–Vink notation):

$$CeO_2 \xrightarrow{TiO_2} Ce_{Ti}^{x} + 2O_o^{x} \quad (2)$$

Figure 1 shows SEM micrographs for $Ti_{1-x}Ce_xO_2$ films annealed at 450 °C for 15 min. It can be seen that the films are very porous and exhibit the well-known cracked-mud morphology. As the amount of $CeO_2$ is increased there is an increase in the crack density and the morphology changes. The micrographs show that the 0.10 mol% $CeO_2$ electrode has islands with small cracks; in the 0.25 mol% $CeO_2$, the cracks among the islands are apparently deeper and, finally, for 0.50 mol% $CeO_2$ the boundaries among the islands lose definition. Probably, the original islands are divided into smaller ones. In light of these observations it can reasonably be expected that an increase in the surface area occurs as the $CeO_2$ content is increased.

Figure 2 shows the cyclic voltammograms for Ti/$Ti_{1-x}Ce_xO_2$ in 0.50 mol dm$^{-3}$ $H_2SO_4$ aqueous solution. In the potential range of 0.0 to −0.2 V almost no current density can be observed. For potentials more negative than −0.2 V, an exponential increase in the current density can be observed, which can be related to reduction of $Ti^{4+}$ sites on the oxide electroactive surface. For more negative potentials than −0.55 V, the $H^+$ reduction occur leading to the detachment of oxide film, possibly due to the pressure of $H_2$ bubbles inside the oxide pores [13]. One fact that supports the hypothesis that $Ti^{4+}$ reduction is the main reaction at potentials more positive than −0.55 V is that an oxidation process

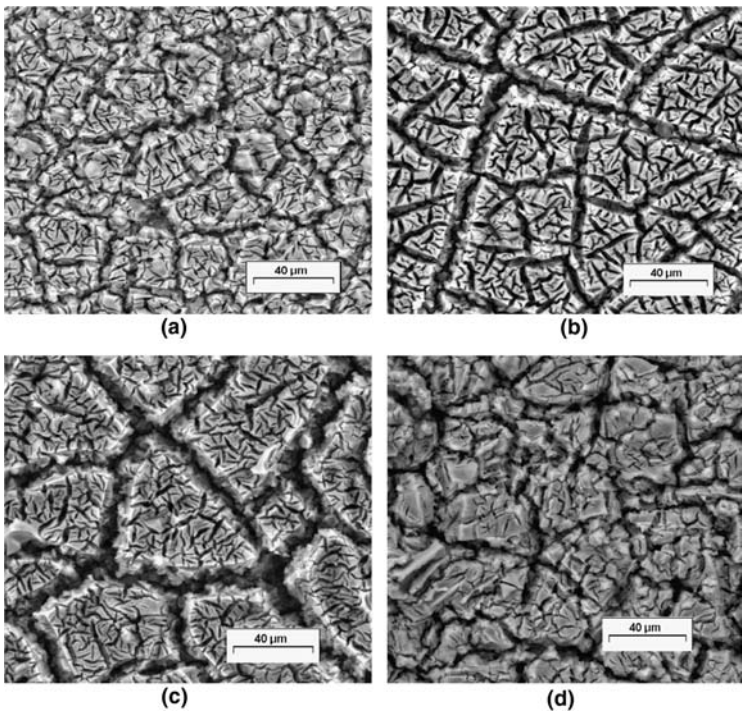


*Fig. 1.* Micrographs of $Ti/Ti_{1-x}Ce_xO_2$ electrodes annealed at 450 °C for 15 min: (a) $x = 0.00$ mol%, (b) $x = 0.10$ mol%, (c) $x = 0.25$ mol%, and (d) $x = 0.50$ mol%.

occurs (with peak potential at −0.47 V) when the sweep is reversed and the ratio between the cathodic and anodic charges is one. If hydrogen evolution occurs it would be expected that the anodic charge was smaller that the cathodic one, due to the reoxidation of $Ti^{3+}$.

Figure 3 displays cyclic voltammograms of the $Ti/Ti_{0.995}Ce_{0.05}O_2$ electrode in 0.50 mol $dm^{-3}$ $H_2SO_4$ solution in the presence of different nitrobenzene (NB) concentrations. An important feature of this figure is the fact that, as the nitrobenzene concentration increases, the cathodic charge is substantially higher than the anodic charge, Figure 3 (inset). This was explained by the mechanism presented in Equation 1 by Ravichandran et al. [10]. According to these authors, the $Ti^{4+}$ sites are reduced to $Ti^{3+}$. In a second step, the $Ti^{3+}$ site is oxidized, transferring one electron to an NB molecule. Then, these $Ti^{4+}$ sites are reduced again. Therefore, when the sweep direction is reversed, the number of $Ti^{3+}$ sites, which can be oxidized, is always lower than the total cathodic charge.

The current change observed could be related to both electronic and geometric factors. The former are those related to the chemical structure of the surface while the latter are those related to the real surface area. Trasatti [19] has referred to the voltammetric charge, $q^*$, as a fingerprint of the surface state of oxide electrodes. The voltammetric charge can be taken to be proportional to

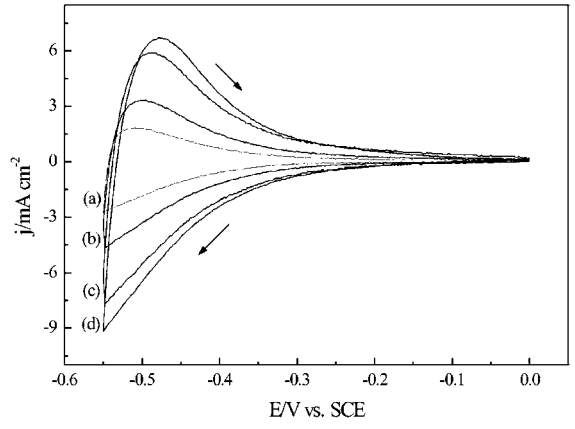


*Fig. 2.* Cyclic voltammograms of $Ti/Ti_{1-x}Ce_xO_2$ electrodes in 0.50 mol $dm^{-3}$ $H_2SO_4$ at 0.05 V $s^{-1}$. $T = 25$ °C. (a) $x = 0.00$ mol%, (b) $x = 0.10$ mol%; (c) $x = 0.25$ mol% and (d) $x = 0.50$ mol%.

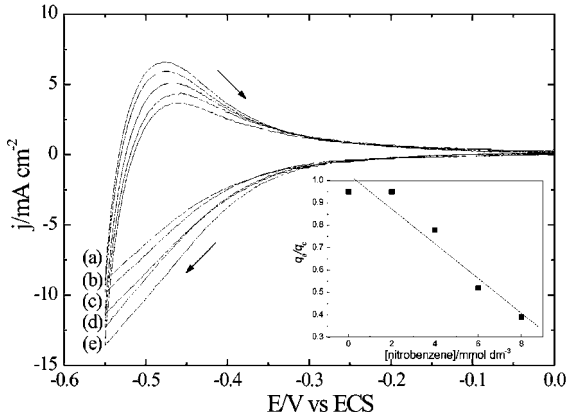


*Fig. 3.* Cyclic voltammograms of $Ti/Ti_{0.995}Ce_{0.005}O_2$ electrodes in 0.50 mol $dm^{-3}$ $H_2SO_4$ aqueous solution at 0.05 V $s^{-1}$. $T = 25$ °C. Nitrobenzene concentrations: (a) 0.0 mmol $dm^{-3}$; (b) 2.0 mmol $dm^{-3}$; (c) 4.0 mmol $dm^{-3}$; (d) 6.0 mmol $dm^{-3}$; (e) 8.0 mmol $dm^{-3}$. Inset: Ratio between anodic and cathodic charges as a function of nitrobenzene concentration.

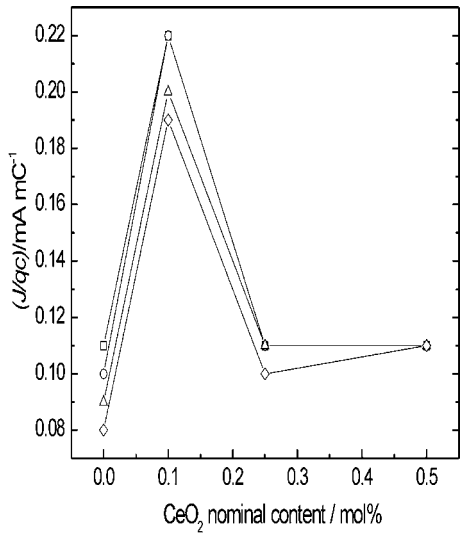


*Fig. 4.* Current density at $E = 0.4$ V (SCE) normalized to unit surface charge for $Ti/Ti_{1-x}Ce_xO_2$ electrodes (0.05 V $s^{-1}$) as a function of $CeO_2$ content. Nitrobenzene concentrations: (□) 0 mmol $dm^{-3}$; (○) 2 mmol $dm^{-3}$; (△) 4 mmol $dm^{-3}$; (◇) 8 mmol $dm^{-3}$. Solution 0.50 mol $dm^{-3}$ $H_2SO_4$ ($V = 0.05$ V $s^{-1}$. $T = 25$ °C).

the active surface area of the electrode, thus providing a method to monitor *in situ* the surface state of oxide layer. Therefore, the current divided by the the cathodic charge is an effective method to discriminate between the electronic and geometric factors. These data are presented in Figure 4.

The normalized activity increases to a maximum value for the electrode with 0.10 mol% of $CeO_2$, then it decreases and remains approximately constant for higher $CeO_2$ contents. The replacement of $Ti^{4+}$ by $Ce^{4+}$ increases the surface area, whereas in fact the true electrocatalytic activity increases only up to 0.10 mol% of $CeO_2$. Figure 4 shows that the addition of 0.10 mol% of $CeO_2$ increases the activity of electrode. At higher $CeO_2$ contents the activity decreases and becomes constant. Therefore, geometric effects are the main ones for amounts of $CeO_2$ higher than 0.10 mol%. This result can be associated with structural factors. It was observed by XRD that a progressive break in the regular periodicity of the $TiO_2$ crystal lattice takes place as the amount of $CeO_2$ increases.

Aniline yields for cathodic reduction of 6.0 mmol $dm^{-3}$ nitrobenzene were determined using $Ti/Ti_{1-x}Ce_xO_2$ electrodes, in 0.50 mol $dm^{-3}$ $H_2SO_4$ aqueous solution, using 10 mA $cm^{-2}$ current density for 10 h, at 50 °C (± 1 °C). The total charge passed during the electrolysis was 344.52 °C. In order to improve the experimental conditions, the nitrobenzene electrolysis was carried out under stirring. The advantage of applying hydrodynamic conditions is that a steady state is reached quickly. The reaction products were characterized using gas chromatography and the results show that the main product of electroreduction is aniline. Table 2 shows the aniline yields and the variation in the yields as $CeO_2$ is added to the $TiO_2$ films.

*Table 2.* Aniline yields and their variation for the cathodic reduction of 6.0 mmol $dm^{-3}$ nitrobenzene at 10 mA $cm^{-2}$ at 50 °C

| $Ti_{1-x}Ce_xO_2$ Electrodes | Aniline yield /% | Variation in aniline yield /Δ% |
|---|---|---|
| $x = 0.00$ mol% | 47.50 (± 3.54) | 0.00 |
| $x = 0.10$ mol% | 52.00 (± 2.83) | 9.47 |
| $x = 0.25$ mol% | 69.15 (± 1.63) | 45.58 |
| $x = 0.50$ mol% | 74.5 (± 2.12) | 56.84 |

A significant increase in the aniline yields is observed as the $CeO_2$ content is increased. The electrode with the lowest crystallite size (10 nm), $Ti/Ti_{0.995}Ce_{0.005}O_2$, presented the best response for electroreduction of nitrobenzene to aniline.

## 4. Conclusions

A $Ti/Ti_{1-x}Ce_xO_2$ electrode has been developed for the electroreduction of nitrobenzene. As a model system, the effect of the $CeO_2$ content on the reduction of nitrobenzene to aniline was investigated. A 58% increase in the aniline yield was observed as the $CeO_2$ concentration increased. These results can be related to both electronic and geometric factors.

## Acknowledgements

The authors gratefully acknowledge CAPES, PADCT-III, and FAPESP of Brazil for financial support.

## References

1. H.B. Beer, *J. Electrochem. Soc.* **127** (1980) 303C.
2. Nidola, *In* S. Trasatti, (ed.), *Electrodes of Conductive Metallic Oxides*, Part B, (Elsevier, Amsterdam, 1981).
3. C. Comninellis and G.P. Vercesi, *J. Appl. Electrochem.* **21** (1991) 335.
4. L.A. De Faria, J.F. Boods and S. Trasatti, *Electrochim. Acta* **37** (1992) 2511.
5. S. Trasatti, In Lipkowski J and Ross, PN (eds.), The Electrochemistry of Novel Materials, (VCH, Weinheim, 1994).
6. C. Ravichandran, S. Chellammal and P.N. Anantharaman, *J. Appl. Electrochem.* **19** (1989) 465.
7. C. Ravichandran, M. Noel and P.N. Anantharaman, *J. Appl. Electrochem.* **26** (1996) 195.
8. C. Ravichandran, D. Vasudevan and P.N. Anantharaman, *J. Appl. Electrochem.* **22** (1992) 1192.
9. C. Ravichandran, M. Noel and P.N. Anantharaman, *J. Appl. Electrochem.* **24** (1994) 1256.
10. C. Ravichandran C.J. Kennady, S. Chellammal, S. Thangavelu and P.N. Anantharaman, *J. Appl. Electrochem.* **21** (1991) 60.
11. M. Noel, P.N. Anantharaman and H.V.K. Udupa, *J. Appl. Electrochem.* **12** (1982) 291.
12. M. Noel, C. Ravichandran and P.N. Anantharaman, *J. Appl. Electrochem.* **25** (1995) 690.
13. C.M. Ronconi and E.C. Pereira, *J. Appl. Electrochem.* **31** (2001) 319.
14. M. Pechini, US Patent No. 3 330 697, 1967.
15. C. Moure, D. Gutierrez, J. Tartaj and P. Duran, *J. Eur. Ceram. Soc.* **23** (2003) 729.

16. V.A. Alves, L.A. Silva and J.F. Boodts, *Electrochim. Acta* **44** (1998) 1525.
17. B.D. Cullity, Elements of X-ray Diffraction, 3rd edn., (Addison-Wesley, Massachusets, 1967).
18. E.R. Leite, A.P. Maciel, I.T. Weber, P.N. Lisboa-Filho, E. Longo, C.O. Paiva-Santos, A.V.C. Andrade, C.A. Paskocimas, Y. Maniette and W.H. Schreiner, *Adv. Mat.* **14** (2002) 905.
19. S. Trasatti, *Electrochim. Acta* **36** (1991) 225.